Journal of Hazardous Materials 494 (2025) 138662

Contents lists available at ScienceDirect

Journal of Hazardous Materials

journal homepage: www.elsevier.com/locate/jhazmat

Measurement and modelling of sorbent-amendment impacts on seasonal and long-term PFAS transport through unsaturated soil lysimeters

Michel Hubert [a,b,*,1], Björn Bonnet [c,1], Sarah E. Hale [b,d], Erlend Sørmo [b,e], Gerard Cornelissen [b,e], Lutz Ahrens [c], Hans Peter H. Arp [a,b]

[a] Norwegian University of Science and Technology (NTNU), Trondheim NO-7491, Norway
[b] Norwegian Geotechnical Institute (NGI), Oslo NO-0806, Norway
[c] Swedish University of Agricultural Sciences (SLU), P.O. Box 7050, Uppsala SE-75007, Sweden
[d] DVGW-Technologiezentrum Wasser, Karlsruhe 76139, Germany
[e] Norwegian University of Life Sciences (NMBU), 1430 Ås, Norway

HIGHLIGHTS

- Waste derived biochars reduced long-chain PFAS leachate by > 99 %, short-chain by 83–96 %.
- Sludge biochars reduced long-chain PFAS leaching as much as commercial sorbents.
- PFAS sorption to sorbents depended on pore-size distribution and surface charge.
- Variable saturated conditions impacted PFAS retention after amendment less.
- A simplified 1D-box model predicted long-term stabilization for biochar amendment.

GRAPHICAL ABSTRACT

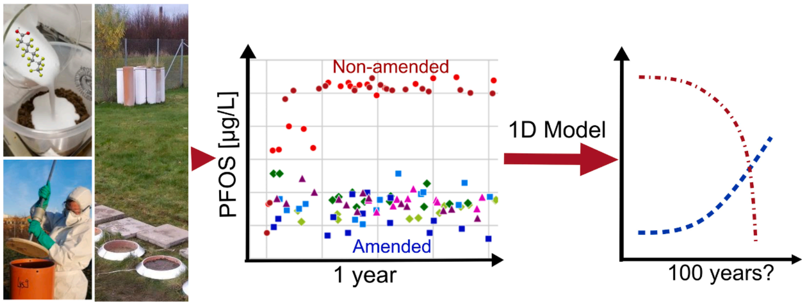

ARTICLE INFO

Keywords:
PFAS
Remediation
Field study
Unsaturated zone
Lysimeter
1D-Box modelling
Air-water interface sorption

ABSTRACT

This study investigated the effectiveness of waste-derived biochar amendments and commercial sorbents in stabilizing PFAS-spiked soils in field-scale *in situ* lysimeters over nearly one year under seasonal changes in Sweden. All tested sorbent amendments reduced average PFAS leachate concentrations by over 99 % for long-chain and 83–96 % for short-chain PFCAs and PFSAs, even under fluctuating water levels. Sewage sludge-derived biochar performed comparably to tested commercial sorbents. Long-chain PFAS remained evenly distributed in the soil, while short-chain PFAS accumulated in lower sections due to higher mobility. Higher PFAS leaching occurred in the spring due to snowmelt events and during summer months due to heavy rainfall. A 1D-transport model was developed to derive retardation factors and identify the fraction sorbed at the air-water interface before and after treatment, as well as PFAS leaching over 100 years. In no-sorbent lysimeters, 30–65 % of perfluorooctane sulfonate (PFOS) was retained at the air-water interface, with seasonal variations of up to 20 %. Inclusion of the sorbent reduced air-water interface effects, as solid-phase sorption became dominant. Over 100 years, nearly all PFOS are predicted to leach from no-sorbent lysimeters, while less than 1 % will leach from

---

[*] Corresponding author at: Norwegian University of Science and Technology (NTNU), Trondheim NO-7491, Norway.
E-mail address: Michel.Hubert@ngi.no (M. Hubert).

[1] Equal first authors

https://doi.org/10.1016/j.jhazmat.2025.138662

soil treated with sewage sludge- derived biochar. Such sorbent amendments can be integrated into ongoing remediation projects.

1. Introduction

Due to their widespread use and persistence, per- and polyfluoroalkyl substances (PFAS) are detected in many regions at concentrations exceeding local risk threshold limit values for diverse environmental media, including soil and groundwater [8,12]. In the last two decades significant efforts have been made, especially in the United States, China, Europe, South Korea, Japan, and in parts of South-East Asia, to map existing PFAS contamination in diverse media, particularly for groundwater and soil [1]. For example, the “forever remediation” project identified that there are more than 2000 hot spots contaminated PFAS sites (>100 ng/L) in Europe, including fire-fighting training facilities at airports, military bases and industrial facilities [12]. These sites often have soil concentrations that are orders of magnitude higher than soils that are considered to represent background concentration levels [8]. Soils contaminated with PFAS can leach to groundwater, where they can impact drinking water resources [5].

Traditional methods of groundwater remediation (e.g. pump and treat, in-situ bioremediation) are often ineffective for PFAS removal due to their high persistence, low volatility, their amphiphilic molecule structure and their relatively high mobility [70]. Immobilization technologies, aiming to stabilize PFAS within the soil and thereby prevent PFAS leaching, are a promising in-situ soil remediation strategies to protect groundwater [15,56]. Soil stabilization offers several advantages relative to other remediation methods, particularly its applicability to various soil types, including cohesive soils, for which other field-tested remediation techniques, such as soil washing, have shown reduced efficiency [69]. Stabilization can be used for both low and high levels of PFAS contamination [36], including a way for hotspot areas that may not be prioritized. The use of sorbents not only reduces leaching from soil but can also be applied for example to biosolids [67]. Additionally, sorbents can be combined with cement for use in stabilization and solidification projects, enhancing the geotechnical stability of the soil when needed [81]. Soil stabilization can also provide immediate protection for critical infrastructure, such as drinking water wells, when deployed in situ within a permeable reactive barrier [65]. Globally, the application of soil stabilization to reduce leaching is increasing, as it is considered a straightforward, sustainable, and cost-effective approach. Hurst et al. [36] argued that soil stabilization using commercial sorbents can be as cost-effective as soil washing, while the use of biochar can further reduce costs [95], making this method a cheaper alternative to landfilling and thermal destruction [36].

Stabilization methods, especially with carbon-based materials, have been successfully applied at the laboratory scale using batch tests [3,39,81] or saturated soil columns [63,84] and more recently have been demonstrated in the field [58]. A concern with conventional carbon-based sorbents, such as activated carbon from anthracite, is their high carbon footprints [86]. This has led to an increasing interest in carbon-based sorbents from more sustainable sources, such as biochar-based sorbents derived from organic waste [85]. Such biochar can be produced and used in the soil with net negative greenhouse gas emissions, as biochars do not decompose and release carbon to the atmosphere like the organic waste feedstock but are rather sequestered for long time scales in the soil providing a carbon sink [59]. For PFAS-contaminated organic wastes, such as sewage sludge from wastewater treatment plants receiving PFAS contaminated water, pyrolysis and subsequent use of the sewage-sludge biochar as sorbents can be a viable and safe waste management strategy [82]. The addition of biochar to soil can also improve the soil’s properties, increasing the availability of nutrients and the soil water holding capacity among other parameters [68,78]. So far there is only a limited number of laboratory scale studies that investigate the efficacy of organic waste derived biochar for PFAS stabilization in soil [43,84,85]. A detailed, field scale analysis of the transport behaviour of PFAS in the unsaturated zone after sorbent amendment with carbon-based sorbents is currently lacking.

The mechanistic processes of PFAS immobilization in soils after the application of biochar are complex and can be influenced by different factors such as climate, soil properties, and biochar characteristics [80]. PFAS sorption is dependent on chemical properties like the perfluorinated chain-length or functional group [84]. Due to their chemical structure, many long-chain PFAS [66] exhibit surfactant behaviour, lowering the interfacial tension and leading to an accumulation at the air-water interface [42]. Previous studies have shown that sorption to the air-water interface can account for $> 50\,\%$ of the total retardation observed for perfluorooctane sulfonate (PFOS) and perfluorooctanoic acid (PFOA) in unsaturated soil [6,54]. Hence, seasonal changes in soil water content in the unsaturated zone, driven by varying atmospheric conditions, will affect the leaching behaviour of PFAS [2,30] and it is crucial to include these sorption processes to correctly model the transport of PFAS in the unsaturated zone [24,51]. However, there is currently a knowledge gap related to how sorbent amendments alter the soil hydrology and associated PFAS retardation mechanisms.

Therefore, this study evaluated the stabilization efficacy for 18 PFAS, with a variety of chain lengths and head groups, in aqueous film forming foam (AFFF) spiked, unsaturated soil using different sorbent amendments in large-scale lysimeters for one year. The specific research objectives were to, a) compare the efficacy of waste-derived biochars and commercial fossil-based sorbents in reducing PFAS leaching from AFFF-contaminated, unsaturated soil, b) test if a 1D-Box model approach, incorporating sorption processes at the air-water interface, can accurately simulate PFAS retention and can be used to predict long-term PFAS leaching and mass retention, and c) evaluate the impact of the air-water interface and PFAS chain length on retention after sorbent amendment. This is the first long-term field lysimeter study using biochar sorbents to stabilize PFAS in soil and to model the long-term efficacy of sorbent amendments in the unsaturated zone.

2. Materials and methods

2.1. Soil

The soil used in this lysimeter study was a loamy sand with a low SOM content ($1.0 \pm 0.1\,\%$) and a soil pH of 4.36 ± 0.02 (0.01 M $CaCl_2$) taken from the B horizon (40 − 160 cm depth) of a remote agricultural field, 17 km south of Uppsala, Sweden (59.733 N, 17.667 E) (Figure S1). The soil showed an average water content of 13.6 % before packing. Before using the soil in the lysimeter, it was stored outdoors covered with a tarp for less than one week.

2.2. Sorbents

In this study four different sorbents were used including two commercially available activated carbon products and two waste-derived biochars as summarized in Table 1. The two commercially available products were a pulverized version of Filtrasorb® 400 (Calgon Carbon, USA) (hereafter referred to as PAC) and RemBind® 100 (Rembind, Australia) (hereafter referred to as RemBind® (RB)). The two biochars used differ in their production feedstock, with one produced from waste timber (hereafter referred to as BC-WT), and another one from digested sewage sludge (hereafter referred to as BC-SL).

Information about the pyrolysis process can be found in the SI (S1.1.2). All selected sorbents have previously demonstrated PFAS stabilization capability in soil at bench scale [25,43,81,84].

2.3. PFAS analysis

2.3.1. Target PFAS and chain length classification

The non-contaminated soil was spiked with 18 target PFAS ($PFAS_{18}$) and an additional 4.5 g of an AFFF (ANSULITE Low Viscosity 3 ×3), to simulate more realistic real world AFFF contamination [29]. All target PFAS were purchased from Sigma Aldrich (Germany) and Apollo Scientific (United Kingdom). The following PFAS were spiked: perfluorobutanoic acid (PFBA), perfluoropentanoic acid (PFPeA), perfluorohexanoic acid (PFHxA), perfluoroheptanoic acid (PFHpA), perfluorooctanoic (PFOA), perfluorononanoic (PFNA) and perfluorodecanoic acid (PFDA), perfluoroundecanoic acid (PFUnDA), perfluorododecanoic acid (PFDoDA), pentacosafluorotridecanoic acid (PFTriDA), perfluorotetradecanoic acid (PFTeDA), perfluorobutanesulfonic acid (PFBS), perfluorohexanesulfonic (PFHxS), perfluorooctanesulfonic (PFOS), 4:2, 6:2 and 8:2 fluorotelomer sulfonic acid (X:2 FTS) and perfluorooctanesulfonamide (FOSA). Water and soil samples were analysed for 18 target PFAS. Information about all PFAS and the isotopically labelled internal standard used can be found in the SI (S1.2, Table S1). Furthermore, a detailed description of sample preparation for water and soil samples and target PFAS analysis can be found in the SI (S1.3).

2.3.2. Quality assurance and quality control (QA/QC)

QA/QC protocols including blanks, limits of detection (LOD) and limits of quantification (LOQ) (Table S3) and recoveries (Table S4 and Table S5) were implemented during all experimental and analytical steps. A detailed discussion is provided in the SI (S1.4).

2.4. PFAS soil spiking method

Due to the large amounts of spiked soil required for this experiment (>1000 kg), a low-volume method similar to the one used by Felizeter et al. [19] was used in this study. In short, for each lysimeter 2 kg of wet soil was spiked with the stated 18 target PFAS (salts and liquid standards dissolved in methanol) and the AFFF (Figure S2). A detailed description of the soil spiking protocol, the used AFFF and the calculated spiking concentrations can be found in the SI (S1.5).

The measured initial PFAS concentration in the two no-sorbent lysimeter after mixing and packing was 2792 ± 133.1 µg/kg dry weight (dw) for PFOS (n = 6), 214 ± 65.2 µg/kg dw for the other 16 target PFAS (n = 96) and 108 ± 11.0 µg/kg for FOSA (n = 6). These concentrations are similar to historical AFFF contaminated field soil [25]. Compared to the calculated target spiking concentrations, the measured PFAS concentrations were 14 % higher for PFOS, 8 % higher for FOSA, and 14 % lower for the other 16 target spiked PFAS. Although the spiking protocol was identical for all lysimeters, and thus the initial PFAS concentrations in the soil should have been the same as the soils treated with biochars, particularly L-BC-WT 1 % and L-BC-WT 4 %, exhibited PFAS concentrations in the starting soil that were on average 50 % lower than expected. This may have been due to errors with the PFAS mass in the standards, the spiking procedure and/or matrix effects (for details, see S1.3.3 in SI). The amount quantified in the soil at the start of the experiment was considered the starting concentration. Individual target PFAS concentrations (Table S6) and mass (Table S7) at the start at the end (Table S8) of the experiment for each lysimeter are summarized in the SI.

2.5. Lysimeter experiments

For this study, 9 lysimeters were set up at the lysimeter station at the Swedish University of Agricultural Sciences (SLU) in Uppsala, Sweden. The lysimeter columns, made from polyvinyl chloride (PVC), were 120 cm long and 30 cm wide. The collected soil was first mixed with the 2 kg PFAS spiked wet soil. After homogenization, the sorbent amendments were added. Each lysimeter was packed with a soil mass of approximately 120 kg (for details see S1.6.1). The different lysimeter including acronyms, the used sorbent including applied concentrations and the PFAS spike used are summarized in Table 2.

To prevent any loss of fine material, a gravel filter (height 10 cm) with two distinct grain sizes (1–3 mm and 0.5–2 mm) followed by a fine

Table 2
Clarification of experimental design.

Acronym	Sorbent/description	Sorbent concentration	PFAS Spike
Blank	No-sorbent added, not spiked	none	Not spiked
L-S1 L-S2	No sorbent added, spiked with AFFF and 18 target PFAS, set up un duplicates.	none	Spiked with AFFF and 18 target PFAS using the same MeOH PFAS spike and AFFF
L-BC-WT 1 %	Biochar produced from waste timber (800°C)	1 %	
L-BC-WT 4 %		4 %	
L-BC-SL 1 %	Biochar produced from anaerobic digested sewage sludge (800°C)	1 %	
L-BC-SL 4 %		4 %	
L-PAC 1 %	Filtrasorb 400® (pulverized)	1 %	
L-RB 1 %	RemBind® 100	1 %	

Table 1
Sorbent characteristics of the four different sorbents.

Sorbent		Filtrasorb® 400 (pulverized)[1])	RemBind® 100[3])	BC-WT[2])	BC-SL*[2])
Ash content [%]		6.10 ± 0.11	-	15.5	73.4
CO_2 Sorption (0.3–1.5 nm)	DFT-SA [m^2/g]	-	-	588	202
	DFT-PV [cm^3/g]	-	-	0.16	0.062
N_2 Sorption (>1.5 nm)	BET-SA [m^2/g]	850–1063	464	131	219
	BJH-PV [cm^3/g]	0.135[5])	0.288	0.025	0.133
Average pore size (d) [nm]			1.24	1.4	2.9
Elemental Content	C	89.6 ± 0.22	-	85.1	27.7
	O	5.77 ± 0	-	6.52	34.9
	H	0.21 ± 0.02	-	1.51	1.32
	N	0.25 ± 0.04	-	1.41	0.89
Other Elements	Fe [g/kg]		-	5.0 ± 0.2	81.3 ± 0.6
	Al [g/kg]	1.5 ± 0.5	-	4.1 ± 0.3	150 ± 15.0
ConAC/OC[4])	%	-	-	79 ± 10	85 ± 2
Point of zero charge		6.1[5])	9.1[6])	< 3	< 3

[1] Gensterblum et al. [20], [2]Sørmo et al. [83], [3] Juhasz et al. [39], [4] as determined by benzopolycarboxylic acid (BPCA) [80], Siriwardena et al. [5][79],Stewart [6][87]
* BC-SL is named BC-DSS-2 in the cited references.

metal mesh (0.5 mm) was positioned at the base of each lysimeter column. The lysimeter experiment was conducted from November 13th 2021 to October 30th 2022. Leachate was collected in 5 L polypropylene (PP) bottles equipped with funnels and metal mesh filters (1 mm) to prevent larger particles or debris from entering the samples. The collection bottles were checked each week and when leaching occurred, leachate samples were collected, and excess water was stored for later disposal. After ending the experiment, composite section-wise (20 cm) soil samples (5 samples for each lysimeter) were taken. Soil samples and selected water samples were extracted and analysed for target PFAS. For each lysimeter, the first leachate sample was analysed, followed by samples approximately every three weeks, targeting high and low infiltration periods.

2.6. Additional leachate and soil analysis

In addition to PFAS analyses, leachate samples were analysed for dissolved organic carbon (DOC) (SS-EN ISO 20236:2021), dissolved anions (SS-EN ISO 10304–1:2009, mod.), and cations (SS-EN ISO 17294–2:2016). A representative soil sample from each lysimeter and horizon was taken in triplicate and freeze-dried to validate the final water content and the soil organic matter content (SOM) (S1.6.2). Additionally, composite samples were collected from each lysimeter for soil size distribution analysis using laser diffraction method (LDM) ISO 11277) and for the mineral composition (EN ISO 17923–2:2016). Soil water retention curves for the soils with no sorbents and sorbents added were conducted (duplicates) using pressure plate extractor tests based on ASTM C1699–09 (2015) (S1.6.2).

2.7. Meteorological data

Meteorological data was taken from the climate station Ultuna (Lantmet Nr. 20000, 59.8179°N, 17.6541°E), which is located approximately 100 m from the lysimeter station. For each lysimeter, the water balance was calculated using the infiltration rate derived from measured precipitation, evaporation estimated with the Penman-Monteith combination equation [37], and the collected leaching volumes (S1.7). While the lysimeters were left bare during the experiment, limited weed growth was observed towards the end.

2.8. 1D-Box model

In this study, a first-order geochemical box model, representing the unsaturated soil along the vertical profile of the lysimeter, was used to simulate the long-term effectiveness of sorbent amendments in reducing the PFAS mass leached from the soil. Although previous studies have shown that PFAS transport can be accurately modelled using, for example, finite-element models that solve Richard's equation for unsaturated flow conditions [24,51,77], these models often need a large number of input parameters which necessitate extensive site-specific characterization, making them impractical for many applications or users. The advantage of the simplified 1D-Box model used in this study is that its input parameters, such as effective porosity and bulk density, can be easily derived from ex-situ soil tests or literature values based on soil texture [32]. This makes the model more accessible and practical for problem owners and stakeholders assessing the effectiveness of soil stabilization as a remediation approach. In a recent study Stults et al. [88] showed that a 1D mass model effectively described PFAS leaching from lab-scale unsaturated soil columns with artificial rain, matching the results of a more complex numerical code. Hale et al. [25] and Sørmo et al. [83] applied a 1D model to predict scenarios for a saturated soil system; the model approach was further developed in this study to better represent conditions in the unsaturated zone, including sorption processes at the air water-interface.

The residual PFAS mass (M_{PFAS}, μg) in the soil column for each timestep can generally be described by the following first order decay function:

$$\frac{M_{PFAS}}{dt} = k_{sorb,unsat} \times M_{PFAS} \tag{1}$$

Where $k_{sorb,unsat}$ is described as the advective-transport rate of water through the vadose zone (k_{unsat} [1/T]) divided by the retention factor (R_{PFAS} [-]):

$$k_{sorb,unsat}(t) = \frac{k_{unsat}(t)}{R_{PFAS}(t)} \tag{2}$$

The advective-transport rate is hereby a function of the flux of water which infiltrates [L/T] the soil column and the effective porosity (n_{eff}), which was derived from tracer experiments (S1.8). Snow accumulation and melting circles in winter times were accounted for following the approach described by Larsbo & Jarvis [46], which is further described in the SI (S1.9).

For each PFAS the retardation factor (R_{PFAS} [-]) can be defined as following:

$$R_{PFAS}(t) = 1 + \frac{K_{d,PFAS} \times \rho_{bulk}}{\theta(t)} + \frac{K_{ai,PFAS} \times A_{AWI}(t)}{\theta(t)} \tag{3}$$

where K_d [L/kg)] is the partitioning coefficient between porewater and soil/biochar surface multiplied by the soil bulk density (ρ_{bulk} [kg/m^3]). K_{ai} [cm] is the air-water interface partitioning coefficient multiplied by the air-water interfacial area (A_{AWI} [cm^{-1}]). Both terms are normalized by the water content of the soil (Θ(t)), to link the retardation through sorption at the soil and the air-water interface to the fraction of the pore volume that contains water.

The fraction of PFAS retention associated to the air-water interface (F_{AWI}(t)) is described by the following equation [55]:

$$F_{AWI}(t) = \frac{R_{PFAS}(t) - 1 - \frac{K_{d,PFAS} \times \rho_{bulk}}{\theta(t)}}{R_{PFAS}(t) - 1} \tag{4}$$

The air water interfacial area is hereby calculated using a correlated AQITT (aqueous interfacial tracer tests) based linear approach (Eq. S15) building on the work of [7].

The modelled data was fitted to the calculated mass of PFAS based on the linear interpolated leachate amounts, by adjusting the $K_{d.PFAS}$ and $K_{ai,PFAS}$ by minimising the cumulative squared error using a generalized reduced gradient non-linear solver [47]. For the no-sorbent spiked lysimeters (L-S1 and L-S2), the solver was constrained by a predefined range for $K_{ai,PFAS}$ (Table S9). The apparent log distribution coefficient $K_{d,PFAS}$ was determined using batch test data (Table S10) and additional literature data (Table S11). This approach accounts for potential discrepancies between $K_{d,PFAS}$ values derived from batch tests, where spiked soil material was used immediately after mixing, and apparent $K_{d,PFAS}$ observed under more representative unsaturated field-scale conditions in the lysimeter experiment. The latter may be influenced by soil aging effects on sorption and precursor transformation over time.

For the sorbent lysimeters, the range of $K_{ai,PFAS}$ values derived from the no-sorbent lysimeters was used to estimate apparent $K_{d,PFAS}$ by fitting the model to the measured data. Model validation was performed by calculating the sqaured Pearson correlation coefficients (R^2) and the average relative error between the modelled and measured mass ($Mass_{error,PFAS}$) (S1.9.2). A detailed description of the developed model and the parameter fitting process can be found in the SI (S1.9).

2.9. Normalized accumulated PFAS mass leached over the experimental time

For each lysimeter the normalized accumulated PFAS mass leached ($PFAS_{Mass}$) in % was calculated based on the following equation:

$$PFAS_{Mass} = \frac{\sum_{t}^{0} M_{PFAS\ leached}}{M_{PFAS,init}} * 100\% \tag{5}$$

where $\sum_t^0 M_{PFAS\ leached}$ is the accumulated mass of grouped PFAS in the leachate over time (t), and $M_{PFAS,init}$ is the initial measured soil PFAS mass in each lysimeter.

2.10. Statistical Analysis

To evaluate whether the normalized accumulated PFAS mass leached significantly varied across different lysimeter treatments, the accumulated mass corresponding to an effective pore volume (EPV) between 0.2 (the point of the latest breakthrough) and 0.725 (the maximum EPV reached by all lysimeters) was selected. The data from lysimeters L-S1 and L-S2 were pooled into a single reference group (no sorbent). Prior to statistical testing, the distribution of leaching data within each group was assessed using the Kolmogorov–Smirnov test, which indicated significant deviations from normality ($p < 0.05$). Consequently, pairwise Wilcoxon rank-sum tests (Mann–Whitney U tests) was used to evaluate differences among the six treatment groups. To account for multiple comparisons, Bonferroni–Holm correction was applied to the resulting *p*-values. The analysis were conducted using Matlab R2018b.

3. Results and discussion

3.1. Soil characteristics and soil water retention curves

The average dry bulk density was 1390 ± 51 kg/m^3 (n = 9), indicating a consistent and uniform packing technique. The biochar amendment generally led to a decrease in dry bulk density and an increase in total porosity consistent with findings from other studies [60]. More detailed data about geotechnical soil parameters for each lysimeter after packing (Table S12), particle size distribution, soil organic matter (SOM) measurements (Table S13) and mineral composition of the soil samples taken from each lysimeter (Table S14) can be found in the SI.

Soil water retention curves were plotted for each lysimeter soil material (Figure S8), showing that the sorbent amendments increased the overall water holding capacity. The field capacity (measured at a −3.3 m pressure head – further explanation can be found in the SI S2.1) was 10.0 ± 0.1 % for the soil with no added sorbent, with the highest value observed for L-BC-WT 4 % (13.0 ± 0.7 %). This increase in field capacity was directly proportional to the percentage of biochar added, which is in line with previous studies [64,94]. In contrast, L-BC-WT 1 % displayed different behaviour, exhibiting the lowest field capacity at 9.1 ± 0.2 %.

3.2. Hydrological data and leachate amount

For the duration of the experiment, the measured accumulated rainfall was 504 mm over 347 days. More detailed precipitation, evaporation (Figure S9, Table S15) and snowfall data (Figure S10) can be found in the SI. The average collected leachate volume from all lysimeters investigated in this study was 24.9 ± 3.2 L. The average fraction of pore volume exchanged across all lysimeters was 0.88 ± 0.16. Details of the water balance for each lysimeter are provided in the SI (Table S16). The error in the water balance ranged from −13.6 to 18.8 %, possible reasons for this minor discrepancy is discussed in the SI (S2.2).

Fig. 1 summarises the number of exchanged pore volumes and the calculated infiltrated rain volume over the experimental time. The first leachate for L-S1 and L-S2 were collected 24 days after the start of the experiment (December 7, 2012). During the first 60 days, leaching volumes were overall low, with an exchanged pore volume of less than 0.03.

For the lysimeters treated with 1 % sorbent, the first leachate was collected after 68 days and for the lysimeters treated with 4 % sorbent after 82–97 days, which can be explained by an increased field capacity and porosity due to sorbent amendment (Figure S8) [64,94]. This increase in field capacity, along with the use of dried soil as a spike (2 kg, corresponding to approximately 2 % of the total soil mass [d.w]) and dried biochar (ranging from 1 to 4 kg depending on the lysimeter), explains the observed increased delay in leaching for the treated lysimeter.

At the end of the experiment, the water content increased with depth (Figure S11), being lowest in the top horizon (0–20 cm, 8.4 ± 0.6 %) and highest in the deepest horizon (80–100 cm, 17.5 ± 0.6 %) across all lysimeters. This pattern can be attributed to the free drainage design of the lysimeter study, where a saturated zone is formed at the bottom of the lysimeter, to overcome the matric potential, before water will drain [48].

3.3. Normalized accumulated PFAS mass leached

Fig. 2 shows the accumulated PFAS mass leached, which was normalized to the initially measured mass, in %) per compound group in the lysimeters, plotted against exchanged pore volume (EPV). PFDoDA, PFTriDA, and PFTeDA were not detected above the limit of detection (LOD) in any leachate sample and are not included. Average PFAS concentrations in leachate over the entire experiment are summarized in Table S17, and detailed concentrations are shown in Figure S12.

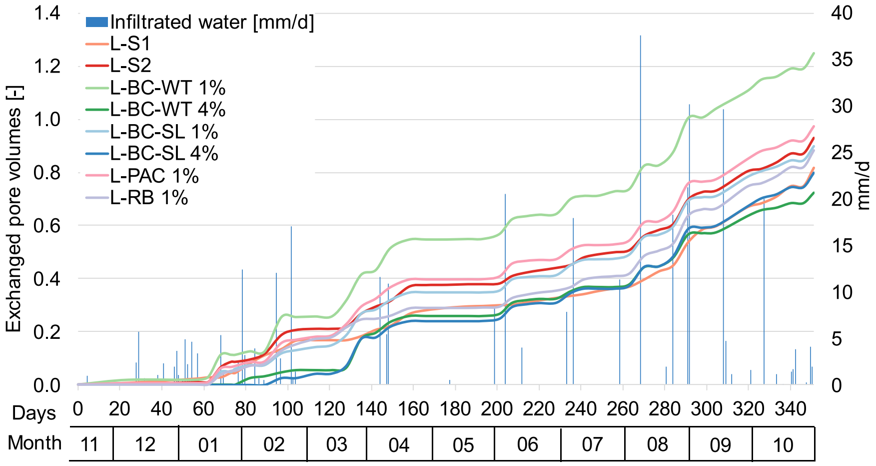

Fig. 1. Exchanged pore volume and precipitation (mm/d) in relation to the run time of the experiment. * Due to missing leachate data for L-PAC 1 % at the start of the experiment, the values were replaced with the average leaching data from the other lysimeter treated with 1 % sorbent.

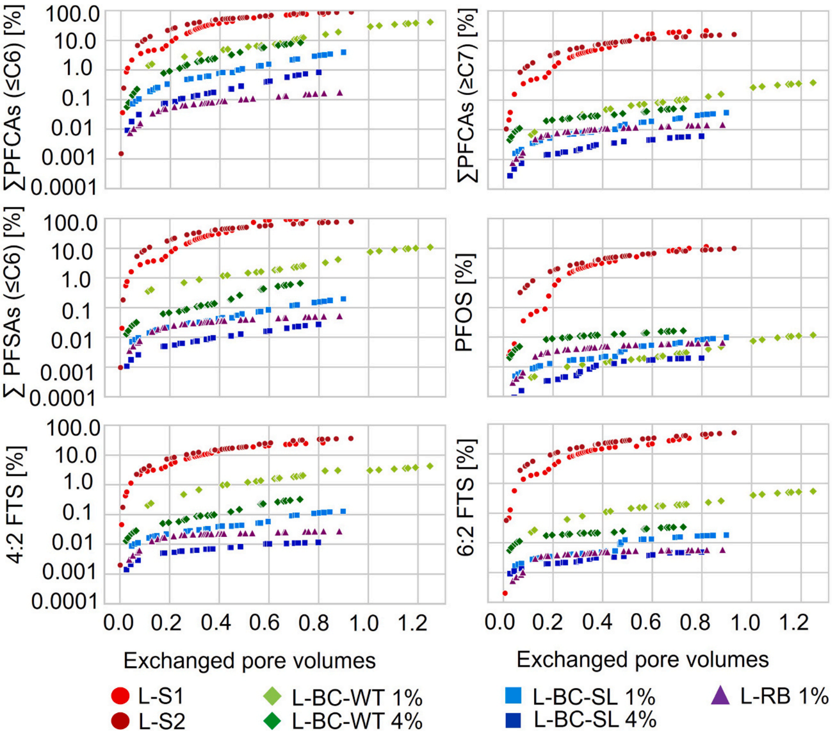

Fig. 2. Accumulated leached PFAS mass normalized to the initial PFAS mass measured for each compound in each lysimeter (log scale) plotted against the exchanged pore volume (EPV). PFAS are grouped based on their fluorinated carbons (e.g. C6 = 6 fluorinated carbons).

The calculated p-values were below 0.05 for nearly all compound groups displayed in Fig. 2, indicating significant differences in PFAS mass leached among the different lysimeter treatments (Figure S14). The only exception was observed for long-chain PFCAs (including all PFCAs from PFOA up to PFUnDA), where the mass leached from L-RB 1 % and L-BC-SL 1 % was not statistically significantly different.

Over the course of the experiment, 77 % and 89 % of the initial mass of short-chain PFCAs (i.e., PFHxA and shorter) leached from L-S1 and L-S2, respectively. Short-chain PFSAs (here grouped as PFBS and PFHxS due to their similar spiked mass) leached in similar patterns, with 98 % from L-S1 and 78 % from L-S2. In comparison, long-chain PFCAs showed lower leached mass fractions, ranging from 16 % in L-S2 to 22 % in L-S1. PFOS exhibited even lower leaching, with 10 % from L-S2 and 11 % from L-S1 by the end of the experiment. Overall, short-chain PFAS leached in higher concentrations and at lower effective pore volumes (EPV) than long-chain PFAS. One exception is 4:2 FTS, which leached in lower mass than its longer-chain analogue 6:2 FTS, likely due to the specific AFFF formulation used, which contained the latter compound (see S1.5.3 in the SI).

In lysimeters treated with the commercial sorbent RemBind®, leaching of long-chain PFAS was below 0.1 % of the initial mass, indicating $>$ 99.9 % stabilization. Only short-chain PFCAs leached in amounts above 0.1 %. For the lysimeter treated with PAC, the accumulated mass leached could not be calculated due to missing early leachate data. However, leachate concentrations (Figure S12) suggest a similarly high retention as observed with RemBind®. This is in line with the study by Bierbaum et al. [4], who observed similar stabilization efficacies of $>$ 99 % for long-chain PFCAs and PFOS and $>$ 90 % for short-chain PFCAs, except for PFBA (16 % and 21 %) in indoor-variably saturated lysimeters treated with 2.5 % of AC-based sorbents similar to the ones used in this study. However, multiple parameters in Bierbaum et al. [4] were different in comparison to the present study such as PFAS concentration and composition, larger L/S ratio, daily irrigation and longer experimental time (30 months).

Among biochar lysimeters long-chain PFCAs, PFOS, 4:2 FTS, and 6:2 FTS leached less than 0.1 % of the initial mass with one exception being L-BC-WT 1 %. Although the accumulated mass leached for 6:2 FTS and long-chain PFCAs from L-BC-WT 1 % was below 1 %, these compounds showed increasing concentrations throughout the experimental time (Figure S12), indicating the lowest sorption capacity for L-BC-WT 1 %. In general, long-chain PFAS were retained more effectively than short-chain PFAS, and short-chain PFCAs were the least stabilized by all sorbents. Notably, L-BC-WT 1 % exhibited the highest leaching of short-chain PFCAs (41 %), while L-BC-SL 4 % showed minimal leaching ($<$1 %). Clear differences were observed among biochars: those derived from waste timber (BC-WT) were less effective over time than those from sewage sludge (BC-SL) for nearly all PFAS. One exception is PFOS, for which the leached mass from L-BC-WT 1 % was lower than for all other biochars and even RemBind®. This may be explained by the unexpectedly low initial PFOS mass (Table S7) and possible preferential flow paths resulting in higher exchanged pore volumes. The findings of the present study align with those of Sørmo et al. [83] who used the same biochars in bench-scale saturated column setups (L/S 0.1–5). In their study, a historically AFFF-impacted sandy soil treated with BC-SL 1 % and BC-WT 1 % showed $>$ 99 % (L/S = 0.2) and 96 % (L/S = 0.5) PFOS leachate reduction and hence mass reduction, respectively, at L/S ratios comparable to those in this study (0.30 for L-BC-WT 1 % and 0.27 for L-BC-SL 1 %). Increasing the biochar content from 1 % to 4 % further reduced PFAS leaching. At an EPV of 0.8, for example, L-BC-SL 4 % leached only 0.8 % of the initial short-chain PFCAs mass, whereas for L-BC-SL 1 % a fivefold increase with 4.0 % leaching of short-chain PFCAs was observed. While sludge-derived biochar at 4 % was slightly less effective than RemBind® and PAC for short-chain PFCAs (Figure S12), it showed comparable or even superior stabilization efficacy for long-chain PFAS (Fig. 2).

3.4. Sorbent properties and sorption mechanistic on PFAS leaching

The high leachate concentrations observed for PFAS from L-S1 and L-S2 can be attributed to the poor sorption properties of the loamy sand (low SOM content) used in this experiment [34]. Higher leachate concentrations with earlier breakthrough and depletion of short-chain PFAS at the end of this study, aligns with the findings of Høisæter et al. [30], who observed faster breakthrough of short-chain PFAS (e.g., PFBS, PFHxA) compared to long-chain PFAS like PFOS when applying AFFF to unsaturated soil columns. Similarly, Lämmer et al. [45] in a 5-year lysimeter study using spiked soil and Bierbaum et al. [4] using PFAS field-contaminated sand (contaminated due to the usage of paper sludge) in their unsaturated indoor lysimeter setup running for 30 months, reported earlier breakthrough and depletion of short-chain PFAS, in their no-sorbent controls. The lower retention of short-chain PFAS is attributed to their shorter fluorinated carbon chain making the PFAS molecule more hydrophilic compared to their longer counter parts, which was shown by different sorption studies before [27,50,62].

Sorption of PFAS to carbon-based sorbents is primarily driven by hydrophobic and electrostatic interactions [17,21,57]. Kabiri et al. [40] studied 28 carbon-based sorbents as soil amendments and highlighted the importance of mesopores (>1.5 nm) and surface charge for PFAS sorption. Their results showed that PFAS removal efficacy increased with the hydrophobicity (fluorinated chain length) of the compound. This aligns with the overall lower retention of short-chain PFAS under unsaturated conditions observed for all tested sorbents in this study. Previous research [43,80,84] has also identified mesopore surface area and corresponding pore volumes as key factors influencing PFAS sorption for the same biochars used in this study. This accounts for the lower sorption affinity of PFAS to waste timber-based biochar (BC-WT) compared to sludge-derived biochar (BC-SL), which exhibits a fivefold higher PFAS-available BJH pore volume and a greater BET surface area (Table 1). Overall, the differences in PFAS leaching reduction among the sorbents tested in this study can be likely attributed to the availability of sorption sites, which increases with pore surface area and volume for pores > 1.5 nm, following the order: BC-WT < BC-SL < RemBind® (RB) < PAC (Table 1).

Electrostatic interactions can also influence PFAS sorption, depending on the point of zero charge (PZC) of the carbon-based sorbents used and the protonation state of the PFAS under investigation [40]. Under typical environmental conditions and given the soil pH of 5.38 ± 0.02 in this study, all PFAS (except some precursors like FOSA) are expected to be negatively charged [34]. While the net surface charge of the biochars used is also expected to be negative (due to a PZC below 3 (Table 1)). PAC (PZC = 6.1) and especially RemBind® (PZC = 9.1), which contains aluminium hydroxide, will have predominantly positively charged surface areas. This enhances PFAS sorption, particularly for short-chain PFAS [96]. These findings align with previous studies suggesting that the presence of positively charged multivalent ions at typical soil pH levels enhances electrostatic interactions with PFAS [11,35,58] and further explains the higher sorption efficacy observed for the two commercially available products compared to the tested biochars, particularly for short-chain PFAS.

3.5. PFAS soil vertical distribution at the end of the experiment

In Fig. 3, the vertical PFAS distribution in the lysimeters at the end of the experiment are presented for selected lysimeters (see Figure S13 in the SI for all lysimeters). L-S1 and L-S2 showed that 84–89 % of the initial mass of PFOS and 57–75 % of long-chain PFCAs were retained in the soil. Shea et al. [76] reported similar retention of 75 % for PFOS in both saturated and unsaturated bench-scale column setups using a AFFF historical contaminated shallow sandy soil from the northeastern US adding the equivalent of 1-year annual rainfall.

In L-S1 and L-S2, the remaining long-chain PFAS were mostly evenly distributed across each 20 cm section. However, in L-S2, long-chain PFAS leached to a greater extent from the bottom of the lysimeter (80–100 cm). In both lysimeters, short-chain PFCAs predominantly accumulated at the bottom (80–100 cm), with nearly all of these compounds leaching from the upper layers. Less than 10 % of the average initial short-chain PFCAs mass in L-S1 and L-S2 remained in the soil, and of that, an average of 87 % was concentrated in the bottom 20 cm of the column for the no-sorbent lysimeter.

Both observations may be explained by the formation of a saturated zone at the bottom of the lysimeter due to the free drainage experimental setup. In sandy soils, such zones can extend up to 30 cm [48]. As

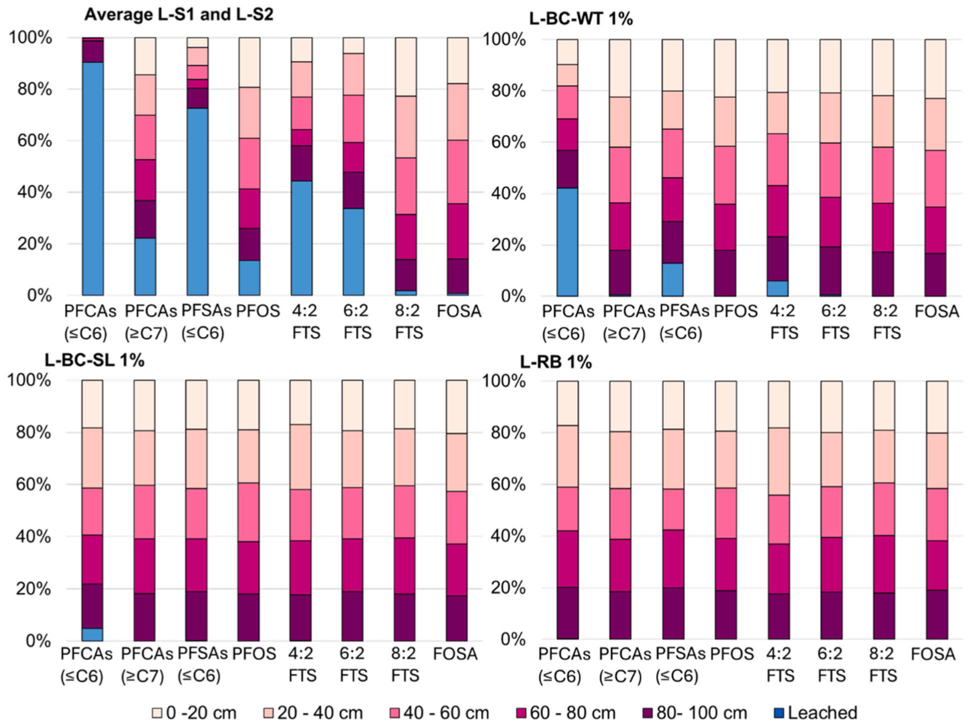

Fig. 3. Vertical distribution at a resolution of 20 cm of PFAS mass in selected lysimeters based on soil analysis before and after the experiment. Relative amount of PFAS mass leached was derived from interpolated leaching samples. Note that no PFAS movement would imply equal distribution in each of the 20 cm boxes, and complete movement would be equal to 100 % of mass leached.

shown in Figure S11, the water content in the 80–100 cm section of L-S1 and L-S2 was approximately 25 %, indicating near-saturated conditions. In these conditions, short-chain, more hydrophilic PFAS accumulated toward the end of the experiment, whereas long-chain PFAS, which are more strongly retained in the unsaturated zone due to sorption at the air-water interface, leached more readily from the bottom where saturated conditions occurred. In contrast, short- and long-chain PFAS were evenly distributed in the sorbent lysimeters at the end of the experiment, indicating that variations in water content within the column had a reduced impact on PFAS transport compared to the no-sorbent lysimeters.

3.6. Fluorine mass balance

For each lysimeter a mass balance was calculated based on the molar fluorine fraction (S2.6 and Table S18). The total fluorine mass balance error ranged between –4 % (L-BC-SL 4 %) to 26 % (L-S1). Losses were observed for terminal perfluoroalkyl acids (PFAAs) towards during the experiment which is likely being caused by measurement uncertainties and data interpolation for the leachate samples. In L-S1 and L-S2, formation of n:2 FTS (with n = 4, 6, 8) was observed up to additional 90.5 % (8:2 FTS in L-S2) and 97.7 % (4:2 FTS in L-S2), as semi-stable intermediate “daughter” compounds during the experiment due to degradation of polyfluorinated “parent” compounds in the used AFFF concentrate. This is a phenomenon which has been commonly reported in AFFF contaminated soils [26,33,93] and is further described in S2.6 in the SI. In lysimeters with sorbents, the fluorine mass balance error for n:2 FTS was less pronounced which could be an indication for lower bioavailability of "parent" compounds and therefore reduced biotransformation due to enhanced sorption.

3.7. Leaching of DOC, anions and cations and heavy metals

Previous studies have indicated a correlation between leaching of DOC and PFAS [29,41,49]. However, the Pearson correlation analysis (Python 3.11) between DOC and individual PFAS (Table S19) revealed weak, significant negative correlations for PFNA (Pearson correlation coefficient (PCC) = -0.65, R^2= 0.42, p = 0.01), PFDA (PCC=-0.56, R^2=0.32, p = 0.02), PFOS (PCC=-0.61, R^2=0.37, p = 0.01) and 6:2 FTS (PCC=-0.60, R^2=0.36, p = 0.01) for L-S2. There was no significant correlation for any of the other PFAS for L-S2 and for any of the PFAS for L-S1, even though all calculated PCC were negative ($p > 0.05$, Table S19). One reason that most PFAS show no significant correlation could be the high concentrations of PFAS in the soil compared to overall low DOC concentrations [41]. The observed negative correlation between PFAS and DOC concentration could be due to the lack of ageing time for the soil, leading to non-equilibrium conditions with low PFAS concentrations in the beginning of the experiment, when DOC leaching is highest (Figure S15).

Increased leaching of anions and cations, particularly SO_4^{2-}, Ca^{2+}, Mg^{2+}, and Na^+, was observed in the lysimeters treated with biochar derived from waste timber (L-BC-WT 1 % and L-BC-WT 4 %) (Table S20). All sorbents reduced metal ion leaching (Fe, Mn, and Al), except for RemBind®, which showed increased leaching, likely due to the incorporated aluminium hydroxide in the sorbent.

Due to the thermal stability of some heavy metals and the low volatilization rates during pyrolysis, waste-derived biochars have been found to potentially contain high concentrations of these compounds [38,84]. In this study, elevated leachate concentrations of Cr were found for the timber-based biochar, with average values of 1.36 ± 0.92 μg/L (n = 4) for L-BC-WT 1 % and 1.85 ± 0.81 μg/L (n = 3) compared to the blank lysimeter, which leached 0.30 ± 0.92 μg/L of Cr (n = 3) (Table S21). The sewage sludge-derived biochar used in this study showed increased leachate concentrations of As with average values of 1.52 ± 0.83 μg/L (n = 4) for L-BC-SL 1 % and 1.80 ± 0.45 μg/L for L-BC-SL 4 % (n = 3), compared to lower leaching from the blank lysimeter (0.51 ± 0.25 μg/L, n = 3). The leached concentrations of Cr and As are still well below the WHO drinking water guideline values (Cr = 50 μg/L, As = 10 μg/L), which are adopted by many countries [91,92]. Therefore, they are not expected to pose a human or environmental risk.

3.8. 1D-Box model verification and limitations

The developed 1D-Box model effectively described PFAS transport in the unsaturated zone and fitted well to the observed data, indicated by overall high R^2 values (Table S22). All lysimeters (except L-RB1 %) showed an average mass error ($Mass_{error,PFAS}$) for all PFAS below 10 % (Table S23). It should be noted that all lysimeters showed non-equilibrium conditions in terms of the hydraulic flow and sorption processes at the beginning of the experiment. To address both effects, a non-equilibrium Q_d value was introduced (Table S24), which was significantly higher than the fitted apparent K_d values observed at later time steps ($p < 0.05$). Apparent log K_d (Table S25), K_{ai} (Table S26) and R_{PFAS} (Table S27), were derived for each PFAS from equilibrium conditions in each lysimeter. It should be noted that for L-S1 and L-S2, the modelled apparent K_d values for long-chain PFAS were higher than those derived from batch tests, whereas for short-chain PFCAs, the apparent K_d values were lower. This discrepancy may to some extent be explained by ongoing precursor transformation over time [4]. In the sorbent lysimeter, apparent K_d values were generally higher than batch test data, likely due to additional aging processes. Measured and modelled values for the residual soil mass of PFOS in L-S1 and L-S2 are shown in Figure S16. The effective porosity (n_{eff}), determined from the salt tracer test (Figure S17) was estimated to be 0.124 ± 0.001 [-] (Table S28), which falls within the range typically observed for medium to silty sand in the literature (n_{eff} = 8–15 %) [32]. In addition, the model accurately described snow accumulation and snow melt in the winter months (Figure S18).

The simplicity of the model approach, requiring fewer parameters for PFAS sorption, unsaturated flow and soil parameters, enhances its applicability for screening the successful applicability of sorbent-amendment strategies. However, this also introduces certain limitations. For contaminated sites containing PFAS precursors, biodegradation rates can only be integrated if transformation pathways are identified [71]. Model limitations and potential improvements are discussed in detail in S2.8.4 in SI.

3.9. Influences of variable saturated conditions on PFAS retention before and after sorbent amendment

As described by Eq. 3, the retardation factor under equilibrium conditions (R_{PFAS}) depends on two time-dependent variables: the soil water content (Θ) and the area of the air-water interface for PFAS, which is directly related to Θ. The water saturation (Figure S19) and consequently the area of the air-water interface (Figure S20) and the fraction of the pore volume that contains water in each lysimeter changed based on the infiltration rate throughout the experiment, which causes the modelled PFAS retardation to vary significantly, particularly in the summer months when strong precipitation events occur. During these periods of high-water infiltration, the modelled retardation is at its lowest. Conversely, at the end of spring, when precipitation is minimal, the water content in the soil columns decreases, leading to the highest levels of modelled PFAS retardation. For example, the overall retardation of PFOS in L-S2 and L-S1 decreased by 39 % and 59 % respectively, between the end of May and the end of August. Variation decreased for PFAS with decreasing fluorinated chain length e.g., the retardation of PFBS decreased by 13 % (L-S2) to 26 % (L-S1). This is consistent with the findings of a field-scale study by Schaefer et al. [74], and a more recent bench-scale column study by Shea et al. [76], both of whom found increased PFAS mobilization under variably saturated conditions for untreated PFAS-impacted soils.

The fraction of PFAS sorbed at the air-water interface (F_{awi}), increased with chain length for both PFCAs and PFSAs (Table S29). In L-S1 and L-S2, the average fraction (± standard deviation) sorbed at the air-water interface for PFOS ranged from 26.5 ± 2.7 % (L-S1) to 65.0 ± 2.7 % (L-S2), whereas for PFBS, the average fraction sorbed was lower, ranging from 11.9 ± 1.5 % (L-S2) to 13.9 ± 2.5 % (L-S1). This chain length dependency is explained by the increased surface activity and stronger sorption at the air-water interface with increasing -CF_2 moiety [10]. The model-derived sorption of PFOS to the air-water interface is hereby in line with previous studies which indicated that sorption to the air-water interface of long-chain PFAS like PFOS or PFOA can contribute to $>$ 50 % of the overall retention [54,6,73].

F_{awi} values and the maximum variation of F_{awi} throughout the one-year experimental time were lower for all sorbent lysimeters than for L-S1 and L-S2 (Table S29 and Figure S21). For PFOS, these changes ranged from 11 % (L-S2) to 20 % (L-S1) over the experimental period, whereas for L-BC-WT 1 %, the change was less than 0.1 %. This is likely due to higher overall apparent K_d values, which indicate that sorption to biochar after treatment is more significant than sorption at the air-water interface. This also suggests that factors such as increased porosity and water retention due to sorbent amendment, which could expand the air-water interface, have a negligible impact on PFAS retardation compared to sorption to the sorbent. Furthermore, changes in the air-water interface area, driven by fluctuations in soil water content, can significantly influence especially long-chain PFAS mass flux from the unsaturated to the saturated zone [54,6,9]. However, due to the reduced significance of the fraction sorbed at the air-water interface in the sorbent lysimeters, seasonal fluctuations in water content, and the resulting release events with high PFAS fluxes due to a collapse of the air-water interface, are likely to be less severe following soil remediation using sorbent amendment. This is in line with the homogenous vertical PFAS soil distribution in all sorbent lysimeters at the end of the experiment (Chapter 3.5).

3.10. Long term efficacy of sorbent amendments

To demonstrate the long-term efficacy of sorbent amendments, the developed 1D-Box model was used to simulate the remaining PFAS mass

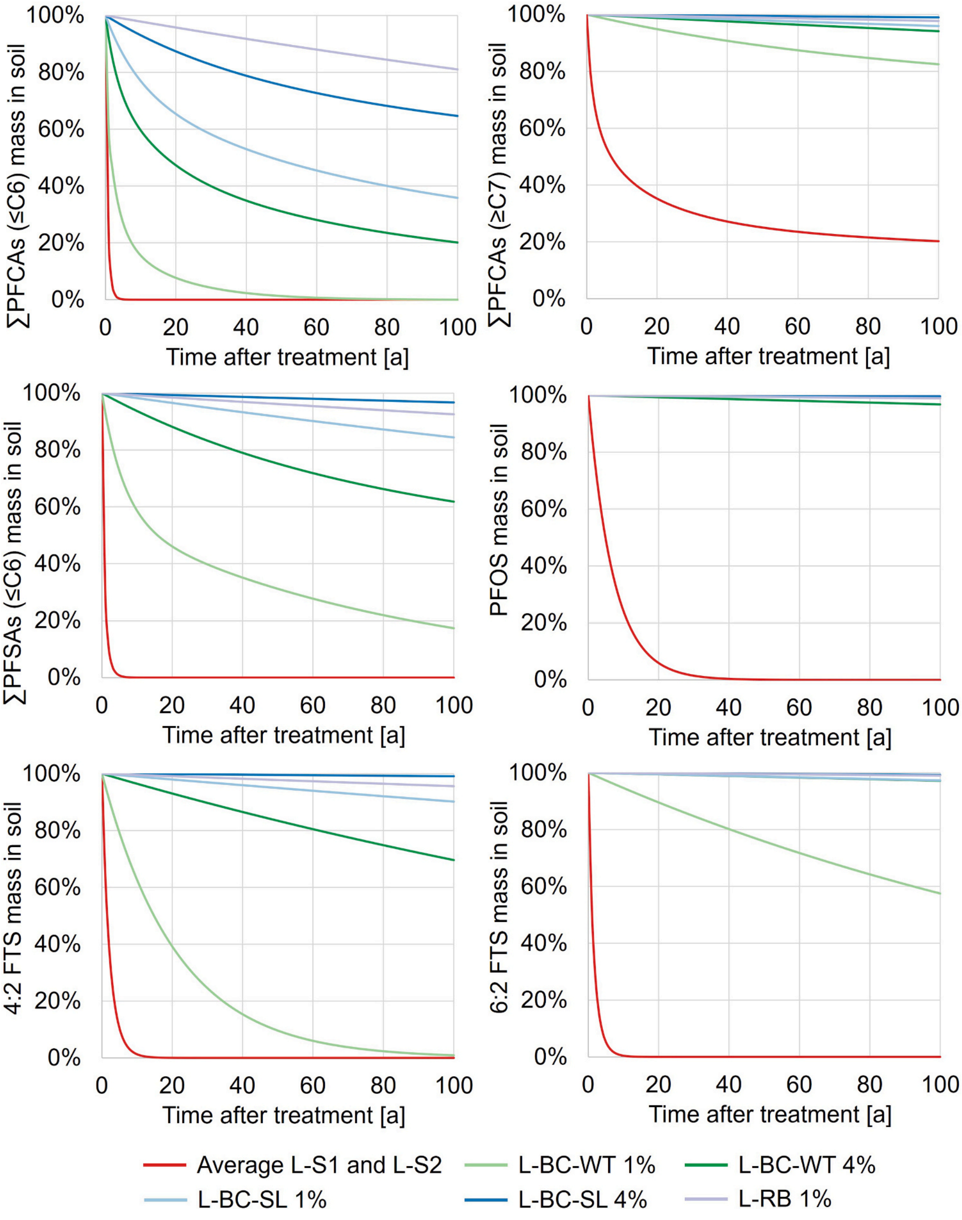

Fig. 4. Modelled remaining PFAS mass in the soil for a time period of 100 years after remediation. No-sorbent (red line) represents the average of L-S1 and L-S2.

[%] in the soil and the associated leachate concentrations [μg/L] over a period of 100 years (Fig. 4 and Table S30). The model was run in yearly time steps where the exponent of the first order decay function ($-k_{sorb.unsat}(t)$) and the infiltration rate ($R_{inf}(t)$) is the average value derived from fitted model data described before. L-S1 and L-S2 are considered as status quo with no remediation measures implemented.

In L-S1 and L-S2, the mass of long-chain PFAS including PFCAs and PFOS show highest leaching in the first 20 years. Only 35 % of the initial mass of long-chain PFCAs, 5.9 % of PFOS and < 0.1 % of 6:2 FTS were retained in the soil column after that time period, implying high mobility and thus a high risk of spreading to recipients. It should be noted that the remaining mass of long-chain PFAS was dominated by PFCAs >C9 (PFDA). Corresponding leachate concentrations after 20 years were still > 100 μg/L for PFOS and respectively > 25 μg/L long-chain PFCAs. More hydrophobic precursors such as 8:2 FTS and FOSA exhibited low overall mass leaching. After 20 years, 67 % of the average initial mass of 8:2 FTS and 86 % of FOSA remained in L-S1 and L-S2. The high retention of precursors, due to their increased sorption at the air-water interface and to the soil matrix, in addition to their potential transformation into terminal PFAS, underscores the long-term burden and risk to underlying groundwater and connected water bodies from AFFF contaminated sites, which was also pointed out in previous investigations [33,71,72]. Short-chain PFAS leached even more quickly and after only 5 years less than 0.8 % of the average initial mass of short-chain PFCAs and short-chain PFSAs was retained in L-S1 and L-S2, with > 90 % of the average original mass leached after 2 years. Corresponding average leachate concentrations after 5 years for short-chain PFCAs and PFSAs were < 5 μg/L (Table S30).

All sorbents effectively stabilized long-chain PFAS in the soil over the 100-year modelled period (Fig. 4). After 100 years, the total mass leached for PFOS ranged from 3.2 % (L-BC-WT 4 %) to < 1 % for L-BC-SL 4 % and for long-chain PFCAs from 27 % (L-BC-WT 1 %) to < 1 % (L-BC-SL 4 %). More hydrophobic precursors such as 8:2 FTS and FOSA, exhibited even lower mass leaching after sorbent amendment. Leachate concentrations for long-chain PFAS were hereby stable for all timesteps, which can be explained by the little change in the mass in the soil column over time. For PFOS, the average concentrations for the more effective sewage sludge-derived biochar ranged from 0.72 ± 0.02 μg/L (at 1 %) to 0.24 ± 0.0003 μg/L (at 4 %).

Short-chain PFAS, which exhibit weaker retention in sorbent soil, also showed promising stabilization efficacy, particularly for L-BC-SL 4 % and L-RB 1 %. After 100 years, 65 % of the initial mass of short-chain PFCAs in L-BC-SL 4 % was still stabilized. For the short-chain PFCAs, the use of RemBind® proved even more effective than that of the biochars, with 81 % of the initial mass still stabilized in the soil after 100 years. PFBA contributed the most to the leaching of short-chain PFAS. Leachate concentrations of short-chain PFAS (Table S30) declined with increasing timesteps, however even after 100 years leachate concentrations for short-chain PFAS were above 1 μg/L.

3.11. Optimizing sorbent amendment for groundwater protection

The proposed changes to the Water Framework Directive, Groundwater Directive, and Environmental Quality Standards Directive suggest a groundwater quality standard for Σ24 PFAS (expressed as PFOA toxicity equivalents) of 4.4 ng/L [16]. From the field- and model results in this study, which used a spiking volume typically found at AFFF-impacted sites, these threshold values would still be greatly exceeded even several decades after sorbent amendment (Table S30). For a successful PFAS stabilization in hotspot soils, such as those simulated here, a reduction of the initial PFAS mass prior sorbent amendment in the soil, with the focus on short-chain PFAS, could be considered depending on the environmental concentration to be met. For instance, soil washing which was tested both ex-situ [23,69] and in-situ at field scale [28] have shown removal of over 90 % of total PFAS including short-chain PFAS, could be done before adding a sorbent amendment, to help protect groundwater resources over a longer timescale.

Several studies have raised concerns about the stability of sorbents, particularly biochar, in soil environments [44,89,90]. Changes to biochar's physical and chemical properties - such as porosity, elemental ratios, and the availability of functional surface groups - can occur over time [14,18,52], potentially impacting PFAS sorption and leaching. Navarro et al. [61] tested various sorbent amendments, including biochar pyrolyzed from hardwood feedstock at high temperatures (750°C), in a batch setup after one week and four years of aging. They found that biochar was less effective at reducing PFAS leaching over time, indicating a negative aging effect on PFAS stabilization, with stabilization efficacy decreasing by at least 22 %. It should be noted that decomposition rates vary depending on the feedstock [90] and that biochar decomposition in soil follows a non-linear pattern, with the highest losses occurring in the first year after application [44,90]. Furthermore, there are ageing effects which can increase stabilisation, for example PFAS can sorb more strongly over time due to soil aging, where PFAS becomes non-accessible in the pore structure [61] and biochar becomes incorporated in soil aggregates whereby pores get blocked [64]. Though there is limited research on the long-term stability of biochar sorbents, some of the previous research available had demonstrated that biochar stability in soil increases with higher pyrolysis temperatures, attributed to the formation of more stable condensed aromatic carbon [89,90]. This means that biochar produced at higher temperatures, like the two biochars tested in this study with high ratios of condensed aromatic carbon (Table 1), are longer lasting in the soil matrix. Furthermore, more hydrophobic PFAS, tend to sorb to these most stable and aromatic regions of the biochar, limiting PFAS leaching [22].

The 1D model was fitted using PFAS leaching data from the first year after stabilization, when the highest decomposition rates are expected to occur, as described above. Consequently, running the model over longer time periods may have overestimated the impact of potential biochar decomposition, rendering the retention factors that are derived conservative with respect to biochar decomposition. However, contrasting this, the biochar may also be more attenuated by dissolved organic matter overtime, occupying sorption sites in competition to PFAS.

The stabilization efficacy of PFAS observed in this lysimeter study was comparable to or higher than results from batch tests [43,85] and saturated soil columns [84], indicating no significant increase in sorption degradation over the one-year period. However, there is a lack of research on the long-term aging effects of waste-derived biochar when used on field-contaminated soils, which need to be addressed in future studies.

This study focused on highly contaminated AFFF sites, such as fire training areas and military bases, where PFAS soil and leachate concentrations are typically much higher than the ppt levels commonly found at other sites for example, agricultural fields where biosolids have been applied [31]. The absence of vegetation in the lysimeters may have influenced PFAS transport in several ways. It limited evapotranspiration, PFAS uptake by plants, and root interactions in the rhizosphere [13]. Microbial activity may also have been altered, both by the lack of vegetation and by the high PFAS concentrations in the soil [75]. These factors could otherwise help reduce vertical PFAS migration. These differences should be considered when interpreting the applicability of the study's findings to sites with different land uses.

4. Conclusion

This study is the first to demonstrate and characterize the effectiveness of waste-derived biochar amendments in stabilizing highly PFAS-contaminated soils impacted by AFFF in a field-scale lysimeter over nearly one year, and the first one to model PFAS leaching based on actual field data in a 100-year perspective. The sludge derived biochar demonstrated similar stabilization efficacy for long-chain PFAS compared to the commercial sorbents tested (RemBind® and Filtrasorb® 400) and was more effective compared to biochar derived from waste timber. Due to its high aromatic content and long-term stabilization potential, biochar produced from sewage sludge shows promise for field-scale applications. However, when used, metal leaching risks should be assessed before implementation [83]. To enhance the sorption of short-chain PFAS to sludge-derived biochars, surface modifications that increase total basicity and raise the point of zero charge could be considered. Examples include ammonia gas treatment [97] or $FeCl_3$-impregnation [53].

The developed 1D-transport model, incorporating sorption at the air-water interface, matched observed data well. For L-S1 and L-S2, higher water content reduced retention at the air-water interface, increasing especially long-chain PFAS fluxes. After sorbent amendment, PFAS sorption to the applied sorbents became the dominant mechanism, effectively mitigating this effect. Over a 100 year modelled period, RemBind® and sludge-derived biochar significantly reduced PFAS leaching. These findings highlight the potential of biochar stabilization as a key component of site remediation strategies. The developed box model and characterization of biochars can be applied to guide the design of future biochar amendment strategies in the unsaturated zone at AFFF-impacted sites.

Environmental implications

This lysimeter study highlights the potential of biochar as a sustainable solution for stabilizing PFAS-contaminated soils, effectively reducing long-chain PFAS leachate concentrations to levels comparable with commercial activated carbon sorbents. Using biochars derived from waste materials as sorbent amendments with net negative greenhouse gas emissions not only addresses PFAS contamination but also contributes to climate change mitigation and presents an opportunity to upcycle problematic waste fractions. The developed box model developed for this study provides a practical tool for designing biochar amendment strategies in the unsaturated zone and promoting soil stabilization efforts at PFAS-contaminated sites.

CRediT authorship contribution statement

Michel Hubert: Writing – review & editing, Writing – original draft, Visualization, Validation, Methodology, Investigation, Formal analysis, Data curation, Conceptualization. **Björn Bonnet:** Writing – review & editing, Writing – original draft, Visualization, Validation, Methodology, Investigation, Formal analysis, Data curation, Conceptualization. **Lutz Ahrens:** Writing – review & editing, Validation, Supervision, Project administration, Investigation, Funding acquisition, Conceptualization. **Sarah Hale:** Writing – review & editing, Supervision, Investigation. **Erlend Sørmo:** Writing – review & editing, Investigation, Data curation. **Gerard Cornelissen:** Writing – review & editing, Investigation. **Hans Peter Arp:** Writing – review & editing, Validation, Supervision, Project administration, Investigation, Funding acquisition, Conceptualization.

Declaration of Generative AI and AI-assisted technologies in the writing process

During the preparation of this work the author(s) used [ChatGPT/OpenAI] in order to improve language. After using this tool/service, the author(s) reviewed and edited the content as needed and take(s) full responsibility for the content of the published article.

Declaration of Competing Interest

The authors declare that they have no known competing financial interests or personal relationships that could have appeared to influence the work reported in this paper.

Acknowledgements

This project received funding from the European Union's Horizon 2020 research and innovation program under the Marie Skłodowska-Curie grant agreement No. 860665 (PERFORCE3 Innovative Training Network), grant agreement No 101036756 (ZeroPM) and grant agreement No 101112723 (Horizon Europe ARAGORN). E.S., G.C. and H.P.H. A. acknowledge co-funding from the Research Council of Norway, through the joint-industry sustainability (BIA-X) project "Valorization of Organic Waste" (VOW) (NFR 299070) and the Miljøforsk project SLUDGEFFECT (NFR 302371). PFAS Analysis was carried out in the Organic environmental chemistry and ecotoxicology (OMK) research lab at SLU, Uppsala Sweden.

Appendix A. Supporting information

Supplementary data associated with this article can be found in the online version at doi:10.1016/j.jhazmat.2025.138662.

Data Availability

Data will be made available on request.

References

[1] Ackerman Grunfeld, D., Gilbert, D., Hou, J., Jones, A.M., Lee, M.J., Kibbey, T.C.G., O'Carroll, D.M., 2024. Underestimated burden of per- and polyfluoroalkyl substances in global surface waters and groundwaters. Nat Geosci 17 (4), 340–346. https://doi.org/10.1038/s41561-024-01402-8.

[2] Adegbule, A.O., Kibbey, T.C.G., 2022. The influence of evaporation and seasonal effects on the water content in the unsaturated zone: a multi-year laboratory study. Water 14 (20), 3294. https://doi.org/10.3390/w14203294.

[3] Barth, E., McKernan, J., Bless, D., Dasu, K., 2021. Investigation of an immobilization process for PFAS contaminated soils. J Environ Manag 296, 113069. https://doi.org/10.1016/j.jenvman.2021.113069.

[4] Bierbaum, T., Klaas, N., Braun, J., Nürenberg, G., Lange, F.T., Haslauer, C., 2023. Immobilization of per- and polyfluoroalkyl substances (PFAS): comparison of leaching behavior by three different leaching tests. Sci Total Environ 876, 162588. https://doi.org/10.1016/j.scitotenv.2023.162588.

[5] Bolan, N., Sarkar, B., Yan, Y., Li, Q., Wijesekara, H., Kannan, K., Tsang, D.C.W., Schauerte, M., Bosch, J., Noll, H., Ok, Y.S., Scheckel, K., Kumpiene, J., Gobindlal, K., Kah, M., Sperry, J., Kirkham, M.B., Wang, H., Tsang, Y.F., Rinklebe, J., 2021. Remediation of poly- and perfluoroalkyl substances (PFAS) contaminated soils – to mobilize or to immobilize or to degrade? J Hazard Mater 401, 123892. https://doi.org/10.1016/j.jhazmat.2020.123892.

[6] Brusseau, M.L., 2018. Assessing the potential contributions of additional retention processes to PFAS retardation in the subsurface. Sci Total Environ 613–614, 176–185. https://doi.org/10.1016/J.SCITOTENV.2017.09.065.

[7] Brusseau, M.L., 2023. Determining air-water interfacial areas for the retention and transport of PFAS and other interfacially active solutes in unsaturated porous media. Sci Total Environ 884, 163730. https://doi.org/10.1016/j.scitotenv.2023.163730.

[8] Brusseau, M.L., Anderson, R.H., Guo, B., 2020. PFAS concentrations in soils: background levels versus contaminated sites. Sci Total Environ 740, 140017. https://doi.org/10.1016/J.SCITOTENV.2020.140017.

[9] Brusseau, M.L., Guo, B., 2022. PFAS concentrations in soil versus soil porewater: mass distributions and the impact of adsorption at air-water interfaces. Chemosphere 302, 134938. https://doi.org/10.1016/j.chemosphere.2022.134938.

[10] Brusseau, M.L., Van Glubt, S., 2021. The influence of molecular structure on PFAS adsorption at air-water interfaces in electrolyte solutions. Chemosphere 281, 130829. https://doi.org/10.1016/J.CHEMOSPHERE.2021.130829.

[11] Campos-Pereira, H., Kleja, D.B., Sjö, C., Ahrens, L., Klysubun, W., Gustafsson, J.P., 2020. The adsorption of per-and polyfluoroalkyl substances (PFASs) onto ferrihydrite is governed by surface charge. Cite This: Environ Sci Technol 54. https://doi.org/10.1021/acs.est.0c01646.

[12] Cordner, A., Brown, P., Cousins, I.T., Scheringer, M., Martinon, L., Dagorn, G., Aubert, R., Hosea, L., Salvidge, R., Felke, C., Tausche, N., Drepper, D., Liva, G., Tudela, A., Delgado, A., Salvatore, D., Pilz, S., Horel, S., 2024. PFAS Contamination in Europe: generating knowledge and mapping known and likely contamination with "expert-reviewed" Journalism. Environ Sci Technol 58 (15), 6616–6627. https://doi.org/10.1021/acs.est.3c09746.

[13] Costello, M.C.S., Lee, L.S., 2020. Sources, fate, and plant uptake in agricultural systems of per- and polyfluoroalkyl substances. Curr Pollut Rep 10 (4), 799–819. https://doi.org/10.1007/s40726-020-00168-y.

[14] Cui, L., Fan, Q., Sun, J., Quan, G., Yan, J., Hina, K., Wang, H., Zhang, Z., Hussain, Q., 2021. Changes in surface characteristics and adsorption properties of 2,4,6-trichlorophenol following Fenton-like aging of biochar. Sci Rep 11 (1), 4293. https://doi.org/10.1038/s41598-021-82129-z.

[15] Darlington, R., Barth, E., McKernan, J., 2018. The challenges of PFAS remediation. Mil Eng 110 (712), 58–60.

[16] European Commission - COM/2022/540 Final (2022).

[17] Fabregat-Palau, J., Vidal, M., Rigol, A., 2022. Examining sorption of perfluoroalkyl substances (PFAS) in biochars and other carbon-rich materials. Chemosphere 302, 134733. https://doi.org/10.1016/j.chemosphere.2022.134733.

[18] Fan, Q., Sun, J., Chu, L., Cui, L., Quan, G., Yan, J., Hussain, Q., Iqbal, M., 2018. Effects of chemical oxidation on surface oxygen-containing functional groups and adsorption behavior of biochar. Chemosphere 207, 33–40. https://doi.org/10.1016/j.chemosphere.2018.05.044.

[19] Felizeter, S., Jürling, H., Kotthoff, M., De Voogt, P., McLachlan, M.S., 2020. Influence of soil on the uptake of perfluoroalkyl acids by lettuce: a comparison between a hydroponic study and a field study. Chemosphere 260, 127608. https://doi.org/10.1016/J.CHEMOSPHERE.2020.127608.

[20] Gensterblum, Y., van Hemert, P., Billemont, P., Busch, A., Charriére, D., Li, D., Krooss, B.M., de Weireld, G., Prinz, D., Wolf, K.-H.A.A., 2009. European interlaboratory comparison of high pressure CO2 sorption isotherms. I: activated carbon. Carbon 47 (13), 2958–2969. https://doi.org/10.1016/j.carbon.2009.06.046.

[21] Ghorbani Gorji, S., Hawker, D.W., Mackie, R., Higgins, C.P., Bowles, K., Li, Y., Kaserzon, S., 2023. Sorption affinity and mechanisms of per-and polyfluoroalkyl substances (PFASs) with commercial sorbents: Implications for passive sampling. J Hazard Mater 457, 131688. https://doi.org/10.1016/j.jhazmat.2023.131688.

[22] Goranov, A.I., Sørmo, E., Hagemann, N., Cornelissen, G., Zimmerman, A.R., Hatcher, P.G., 2024. Using the benzenepolycarboxylic acid (BPCA) method to assess activated biochars and their PFAS sorption abilities. Chemosphere 355, 141750. https://doi.org/10.1016/j.chemosphere.2024.141750.

[23] Grimison, C., Knight, E.R., Nguyen, T.M.H., Nagle, N., Kabiri, S., Bräunig, J., Navarro, D.A., Kookana, R.S., Higgins, C.P., McLaughlin, M.J., Mueller, J.F., 2023. The efficacy of soil washing for the remediation of per- and poly-fluoroalkyl substances (PFASs) in the field. J Hazard Mater 445, 130441. https://doi.org/10.1016/j.jhazmat.2022.130441.

[24] Guo, B., Zeng, J., Brusseau, M.L., 2020. A mathematical model for the release, transport, and retention of per- and polyfluoroalkyl substances (PFAS) in the vadose zone. Water Resour Res 56 (2). https://doi.org/10.1029/2019WR026667.

[25] Hale, S.E., Arp, H.P.H., Slinde, G.A., Wade, E.J., Bjørseth, K., Breedveld, G.D., Straith, B.F., Moe, K.G., Jartun, M., Høisæter, Å., 2017. Sorbent amendment as a remediation strategy to reduce PFAS mobility and leaching in a contaminated sandy soil from a Norwegian firefighting training facility. Chemosphere 171, 9–18. https://doi.org/10.1016/J.CHEMOSPHERE.2016.12.057.

[26] Harding-Marjanovic, K.C., Houtz, E.F., Yi, S., Field, J.A., Sedlak, D.L., Alvarez-Cohen, L., 2015. Aerobic biotransformation of fluorotelomer thioether amido sulfonate (lodyne) in AFFF-amended microcosms. Environ Sci Technol 49 (13), 7666–7674. https://doi.org/10.1021/acs.est.5b01219.

[27] Higgins, C., Richard, L., 2006. Sorpt Perfluorinated Surfactants Sediment † https://doi.org/10.1021/es061000n.

[28] Høisæter, Å., Arp, H.P.H., Slinde, G., Knutsen, H., Hale, S.E., Breedveld, G.D., Hansen, M.C., 2021. Excavated vs novel in situ soil washing as a remediation strategy for sandy soils impacted with per- and polyfluoroalkyl substances from aqueous film forming foams. Sci Total Environ 794, 148763. https://doi.org/10.1016/J.SCITOTENV.2021.148763.

[29] Høisæter, Å., Breedveld, G.D., 2022. Leaching potential of per- and polyfluoroalkyl substances from source zones with historic contamination of aqueous film forming foam - a surfactant mixture problem. Environ Adv 8, 100222. https://doi.org/10.1016/j.envadv.2022.100222.

[30] Høisæter, Å., Pfaff, A., Breedveld, G.D., 2019. Leaching and transport of PFAS from aqueous film-forming foam (AFFF) in the unsaturated soil at a firefighting training facility under cold climatic conditions. J Contam Hydrol 222, 112–122. https://doi.org/10.1016/J.JCONHYD.2019.02.010.

[31] Holly, M.A., Gunn, K.M., Keymer, D., Sanford, J.R., 2024. Evaluation of per- and polyfluoroalkyl substances leaching from biosolids and mitigation potential of biochar through undisturbed soil columns. ACS EST Water 4 (2), 413–426. https://doi.org/10.1021/acsestwater.3c00414.

[32] Hölting, B., Coldewey, W.G., 2019. Hydrogeology. Springer Berlin Heidelberg. https://doi.org/10.1007/978-3-662-56375-5.

[33] Houtz, E.F., Higgins, C.P., Field, J.A., Sedlak, D.L., 2013. Persistence Perfluoroalkyl Acid Precursors AFFF-Impact Groundw Soil. https://doi.org/10.1021/es4018877.

[34] Hubert, M., Arp, H.P.H., Hansen, M.C., Castro, G., Meyn, T., Asimakopoulos, A.G., Hale, S.E., 2023. Influence of grain size, organic carbon and organic matter residue content on the sorption of per- and polyfluoroalkyl substances in aqueous film forming foam contaminated soils - Implications for remediation using soil washing. Sci Total Environ 875, 162668. https://doi.org/10.1016/j.scitotenv.2023.162668.

[35] Hubert, M., Meyn, T., Hansen, M.C., Hale, S.E., Arp, H.P.H., 2024. Per- and polyfluoroalkyl substance (PFAS) removal from soil washing water by coagulation and flocculation. Water Res 249, 120888. https://doi.org/10.1016/j.watres.2023.120888.

[36] Hurst, J., Hale, S., Miles, J., Dal, E., Gevaerts, W., Burdick, J., 2024. PFAS Soil Treat Process - A Rev Oper Ranges Constraints.

[37] Šimůnek, J., S. M. S, M.Š.H., van G, M.Th, 2009. The Hydrus-1D software package for simulating the one-dimensional movement of water. Heat, Mult Solutes Var-Satur Media Version 4 (08).

[38] Jin, J., Li, Y., Zhang, J., Wu, S., Cao, Y., Liang, P., Zhang, J., Wong, M.H., Wang, M., Shan, S., Christie, P., 2016. Influence of pyrolysis temperature on properties and environmental safety of heavy metals in biochars derived from municipal sewage sludge. J Hazard Mater 320, 417–426. https://doi.org/10.1016/j.jhazmat.2016.08.050.

[39] Juhasz, A.L., Kastury, F., Herde, C., Tang, W., 2022. Application of soil amendments for reducing PFAS leachability and bioavailability. Environ Pollut 307, 119498. https://doi.org/10.1016/j.envpol.2022.119498.

[40] Kabiri, S., Navarro, D.A., Hamad, S.A., Grimison, C., Higgins, C.P., Mueller, J.F., Kookana, R.S., McLaughlin, M.J., 2023. Physical and chemical properties of carbon-based sorbents that affect the removal of per- and polyfluoroalkyl substances from solution and soil. Sci Total Environ 875, 162653. https://doi.org/10.1016/j.scitotenv.2023.162653.

[41] Kabiri, S., Tavakkoli, E., Navarro, D.A., Degryse, F., Grimison, C., Higgins, C.P., Mueller, J.F., Kookana, R.S., McLaughlin, M.J., 2024. The complex effect of dissolved organic carbon on desorption of per- and poly-fluoroalkyl substances from soil under alkaline conditions. Environ Pollut 356, 124234. https://doi.org/10.1016/j.envpol.2024.124234.

[42] Krafft, M.P., Riess, J.G., 2015. Selected physicochemical aspects of poly- and perfluoroalkylated substances relevant to performance, environment and sustainability—Part one. Chemosphere 129, 4–19. https://doi.org/10.1016/j.chemosphere.2014.08.039.

[43] Krahn, K.M., Cornelissen, G., Castro, G., Arp, H.P.H., Asimakopoulos, A.G., Wolf, R., Holmstad, R., Zimmerman, A.R., Sørmo, E., 2023. Sewage sludge biochars as effective PFAS-sorbents. J Hazard Mater 445, 130449. https://doi.org/10.1016/j.jhazmat.2022.130449.

[44] Kuzyakov, Y., Bogomolova, I., Glaser, B., 2014. Biochar stability in soil: decomposition during eight years and transformation as assessed by compound-specific 14C analysis. Soil Biol Biochem 70, 229–236. https://doi.org/10.1016/j.soilbio.2013.12.021.

[45] Lämmer, R., Weidemann, E., Göckener, B., Stahl, T., Breuer, J., Kowalczyk, J., Just, H., Boeddinghaus, R.S., Gassmann, M., Kling, H.-W., Bücking, M., 2022. Evaluation of the transformation and leaching behavior of two polyfluoroalkyl phosphate diesters in a field lysimeter study. J Agric Food Chem 70 (45), 14329–14338. https://doi.org/10.1021/acs.jafc.2c03334.

[46] Larsbo, M., Jarvis, N., 2003. MACRO 5.0. A model of water flow and solute transport in macroporous soil. Tech Descr.

[47] Lasdon, L.S., Fox, R.L., Ratner, M.W., 1974. Nonlinear optimization using the generalized reduced gradient method. Rev Française d'automatique, Inform, Rech Opérationnelle Rech OPÉRATIONNELLE 8, 73–103.

[48] Lewis, J., Sjöstrom, J., 2010. Optimizing the experimental design of soil columns in saturated and unsaturated transport experiments. J Contam Hydrol 115 (1–4), 1–13. https://doi.org/10.1016/j.jconhyd.2010.04.001.

[49] Li, J., Sha, H., Liu, W., Yuan, Y., Zhu, G., Meng, F., Xi, B., Tan, W., 2024. Transport of per-/polyfluoroalkyl substances from leachate to groundwater as affected by dissolved organic matter in landfills. Environ Res 247, 118230. https://doi.org/10.1016/j.envres.2024.118230.

[50] Li, Y., Oliver, D.P., Kookana, R.S., 2018. A critical analysis of published data to discern the role of soil and sediment properties in determining sorption of per and polyfluoroalkyl substances (PFASs). Sci Total Environ 628–629, 110–120. https://doi.org/10.1016/J.SCITOTENV.2018.01.167.

[51] Liao, S., Garza-Rubalcava, U., Abriola, L.M., Preisendanz, H.E., Lee, L.S., Pennell, K.D., 2025. Simulating PFAS transport in effluent-irrigated farmland using PRZM5, LEACHM, and HYDRUS-1D models. J Environ Qual 54 (1), 54–65. https://doi.org/10.1002/jeq2.20639.

[52] Liu, Y., Chen, J., 2022. Effect of ageing on biochar properties and pollutant management. Chemosphere 292, 133427. https://doi.org/10.1016/j.chemosphere.2021.133427.

[53] Liu, Z., Zhang, P., Wei, Z., Xiao, F., Liu, S., Guo, H., Qu, C., Xiong, J., Sun, H., Tan, W., 2023. Porous Fe-doped graphitized biochar: an innovative approach for co-removing per-/polyfluoroalkyl substances with different chain lengths from natural waters and wastewater. Chem Eng J 476, 146888. https://doi.org/10.1016/j.cej.2023.146888.

[54] Lyu, Y., Brusseau, M.L., Chen, W., Yan, N., Fu, X., Lin, X., 2018. Adsorption of PFOA at the air–water interface during transport in unsaturated porous media. Environ Sci Technol 52 (14), 7745–7753. https://doi.org/10.1021/acs.est.8b02348.

[55] Lyu, Y., Wang, B., Du, X., Guo, B., Brusseau, M.L., 2022. Air-water interfacial adsorption of C4-C10 perfluorocarboxylic acids during transport in unsaturated porous media. Sci Total Environ 831, 154905. https://doi.org/10.1016/j.scitotenv.2022.154905.

[56] Mahinroosta, R., Senevirathna, L., 2020. A review of the emerging treatment technologies for PFAS contaminated soils. J Environ Manag 255, 109896. https://doi.org/10.1016/j.jenvman.2019.109896.

[57] McCleaf, P., Englund, S., Östlund, A., Lindegren, K., Wiberg, K., Ahrens, L., 2017. Removal efficiency of multiple poly- and perfluoroalkyl substances (PFASs) in drinking water using granular activated carbon (GAC) and anion exchange (AE) column tests. Water Res 120, 77–87. https://doi.org/10.1016/j.watres.2017.04.057.

[58] Mcdonough, J.T., Anderson, R.H., Lang, J.R., Liles, D., Matteson, K., Olechiw, T., 2021. Field-scale demonstration of pfas leachability following in situ soil stabilization, 7, 419–429. https://doi.org/10.1021/acsomega.1c04789.

[59] Morales, M., Arp, H.P.H., Castro, G., Asimakopoulos, A.G., Sørmo, E., Peters, G., Cherubini, F., 2024. Eco-toxicological and climate change effects of sludge thermal treatments: pathways towards zero pollution and negative emissions. J Hazard Mater 470, 134242. https://doi.org/10.1016/j.jhazmat.2024.134242.

[60] Mukherjee, A., Lal, R., 2013. Biochar impacts on soil physical properties and greenhouse gas emissions. Agronomy 3 (2), 313–339. https://doi.org/10.3390/agronomy3020313.

[61] Navarro, D.A., Kabiri, S., Ho, J., Bowles, K.C., Davis, G., McLaughlin, M.J., Kookana, R.S., 2023. Stabilisation of PFAS in soils: Long-term effectiveness of

carbon-based soil amendments. Environ Pollut, 121249. https://doi.org/10.1016/j.envpol.2023.121249.

[62] Nguyen, T.M.H., Brä, J., Thompson, K., Thompson, J., Kabiri, S., Navarro, D.A., Kookana, R.S., Grimison, C., Barnes, C.M., Higgins, C.P., Mclaughlin, M.J., Mueller, J.F., 2020. Influences of chemical properties, soil properties, and solution ph on soil−water partitioning coefficients of per-and polyfluoroalkyl substances (PFASs). Cite This: Environ Sci Technol 54, 15883–15892. https://doi.org/10.1021/acs.est.0c05705.

[63] Niarchos, G., Ahrens, L., Kleja, D.B., Fagerlund, F., 2022. Per- and polyfluoroalkyl substance (PFAS) retention by colloidal activated carbon (CAC) using dynamic column experiments. Environ Pollut 308, 119667. https://doi.org/10.1016/J.ENVPOL.2022.119667.

[64] Obia, A., Mulder, J., Martinsen, V., Cornelissen, G., Børresen, T., 2016. In situ effects of biochar on aggregation, water retention and porosity in light-textured tropical soils. Soil Tillage Res 155, 35–44. https://doi.org/10.1016/j.still.2015.08.002.

[65] Obiri-Nyarko, F., Grajales-Mesa, S.J., Malina, G., 2014. An overview of permeable reactive barriers for in situ sustainable groundwater remediation. Chemosphere 111, 243–259. https://doi.org/10.1016/j.chemosphere.2014.03.112.

[66] OECD, O.For E.C., D, 2018. Toward a new comprehensive global database of Per-and Polyfrluoroalkyl substances (PFASs). Summ Rep Updat OECD 2007 List PFASs.

[67] Openiyi, E.O., Lee, L.S., Alukkal, C.R., 2025. Evaluating sorbents for reducing per- and polyfluoroalkyl substance mobility in biosolids-amended soil columns. J Environ Qual 54 (1), 118–131. https://doi.org/10.1002/jeq2.20658.

[68] Pandit, N.R., Mulder, J., Hale, S.E., Martinsen, V., Schmidt, H.P., Cornelissen, G., 2018. Biochar improves maize growth by alleviation of nutrient stress in a moderately acidic low-input Nepalese soil. Sci Total Environ 625, 1380–1389. https://doi.org/10.1016/j.scitotenv.2018.01.022.

[69] Quinnan, J., Morrell, C., Nagle, | Nathan, Maynard, K.G., 2022. Ex situ Soil Washing Remove PFAS adsorbed Soils Source zones. https://doi.org/10.1002/rem.21727.

[70] Ross, I., McDonough, J., Miles, J., Storch, P., Thelakkat Kochunarayanan, P., Kalve, E., Hurst, J., S. Dasgupta, S., Burdick, J., 2018. A review of emerging technologies for remediation of PFASs. Remediat J 28 (2), 101–126. https://doi.org/10.1002/rem.21553.

[71] Ruyle, B.J., Thackray, C.P., Butt, C.M., LeBlanc, D.R., Tokranov, A.K., Vecitis, C.D., Sunderland, E.M., 2023. Centurial persistence of forever chemicals at military fire training sites. Environ Sci Technol 57 (21), 8096–8106. https://doi.org/10.1021/acs.est.3c00675.

[72] Sadia, M., Kunz, M., ter Laak, T., De Jonge, M., Schriks, M., van Wezel, A.P., 2023. Forever legacies? Profiling historical PFAS contamination and current influence on groundwater used for drinking water. Sci Total Environ 890, 164420. https://doi.org/10.1016/j.scitotenv.2023.164420.

[73] Schaefer, C.E., Lavorgna, G.M., Lippincott, D.R., Nguyen, D., Christie, E., Shea, S., O'Hare, S., Lemes, M.C.S., Higgins, C.P., Field, J., 2022. A field study to assess the role of air-water interfacial sorption on PFAS leaching in an AFFF source area. J Contam Hydrol 248, 104001. https://doi.org/10.1016/j.jconhyd.2022.104001.

[74] Schaefer, C.E., Lavorgna, G.M., Lippincott, D.R., Nguyen, D., Schaum, A., Higgins, C.P., Field, J., 2023. Leaching of perfluoroalkyl acids during unsaturated zone flushing at a field site impacted with aqueous film forming foam. Environ Sci Technol 57 (5), 1940–1948. https://doi.org/10.1021/acs.est.2c06903.

[75] Senevirathna, S.T.M.L.D., Krishna, K.C.B., Mahinroosta, R., Sathasivan, A., 2022. Comparative characterization of microbial communities that inhabit PFAS-rich contaminated sites: a case-control study. J Hazard Mater 423, 126941. https://doi.org/10.1016/j.jhazmat.2021.126941.

[76] Shea, S.M., Schaefer, C.E., Illangasekare, T., Higgins, C.P., 2025. Release of poly- and perfluoroalkyl substances from AFFF-impacted soils: effects of water saturation in vadose zone soils. J Contam Hydrol 269, 104506. https://doi.org/10.1016/j.jconhyd.2025.104506.

[77] Silva, J.A.K., Šimůnek, J., McCray, J.E., 2020. A modified hydrus model for simulating PFAS Transport in the Vadose Zone. Water 12 (10), 2758. https://doi.org/10.3390/w12102758.

[78] Singh Yadav, S.P., Bhandari, S., Bhatta, D., Poudel, A., Bhattarai, S., Yadav, P., Ghimire, N., Paudel, P., Paudel, P., Shrestha, J., Oli, B., 2023. Biochar application: a sustainable approach to improve soil health. J Agric Food Res 11, 100498. https://doi.org/10.1016/j.jafr.2023.100498.

[79] Siriwardena, D.P., Crimi, M., Holsen, T.M., Bellona, C., Divine, C., Dickenson, E., 2019. Changes in adsorption behavior of perfluorooctanoic acid and perfluorohexanesulfonic acid through chemically-facilitated surface modification of granular activated carbon. Environ Eng Sci 36 (4), 453–465. https://doi.org/10.1089/ees.2018.0319.

[80] Skjennum, K.A., Krahn, K.M., Sørmo, E., Wolf, R., Goranov, A.I., Hatcher, P.G., Hartnik, T., Arp, H.P.H., Zimmerman, A.R., Zhang, Y., Cornelissen, G., 2024. The impact of biochar's physicochemical properties on sorption of perfluorooctanoic acid (PFOA). Sci Total Environ 955, 177191. https://doi.org/10.1016/j.scitotenv.2024.177191.

[81] Sörengård, M., Kleja, D.B., Ahrens, L., 2019. Stabilization and solidification remediation of soil contaminated with poly- and perfluoroalkyl substances (PFASs). J Hazard Mater 367, 639–646. https://doi.org/10.1016/J.JHAZMAT.2019.01.005.

[82] Sørmo, E., Castro, G., Hubert, M., Licul-Kucera, V., Quintanilla, M., Asimakopoulos, A.G., Cornelissen, G., Arp, H.P.H., 2023. The decomposition and emission factors of a wide range of PFAS in diverse, contaminated organic waste fractions undergoing dry pyrolysis. J Hazard Mater 454, 131447. https://doi.org/10.1016/j.jhazmat.2023.131447.

[83] Sørmo, E., Dublet-Adli, G., Menlah, G., Flatabø, G.Ø., Zivanovic, V., Carlsson, P., Almås, Å., Cornelissen, G., 2024. Heavy metals in pyrolysis of contaminated wastes: phase distribution and leaching behaviour. Environments 11 (6), 130. https://doi.org/10.3390/environments11060130.

[84] Sørmo, E., Lade, C.B.M., Zhang, J., Asimakopoulos, A.G., Åsli, G.W., Hubert, M., Goranov, A.I., Arp, H.P.H., Cornelissen, G., 2024. Stabilization of PFAS-contaminated soil with sewage sludge- and wood-based biochar sorbents. Sci Total Environ 922, 170971. https://doi.org/10.1016/j.scitotenv.2024.170971.

[85] Sørmo, E., Silvani, L., Bjerkli, N., Hagemann, N., Zimmerman, A.R., Hale, S.E., Hansen, C.B., Hartnik, T., Cornelissen, G., 2021. Stabilization of PFAS-contaminated soil with activated biochar. Sci Total Environ 763, 144034. https://doi.org/10.1016/J.SCITOTENV.2020.144034.

[86] Sparrevik, M., Saloranta, T., Cornelissen, G., Eek, E., Fet, A.M., Breedveld, G.D., Linkov, I., 2011. Use of life cycle assessments to evaluate the environmental footprint of contaminated sediment remediation. Environ Sci Technol 45 (10), 4235–4241. https://doi.org/10.1021/es103925u.

[87] Stewart, R., 2017, May 22. Immobilization and safe disposal of aqueous film forming foam (AFFF) impacted soil in Australia. Bioremediation Symp Proc 2017.

[88] Stults, J.F., Schaefer, C.E., MacBeth, T., Fang, Y., Devon, J., Real, I., Liu, F., Kosson, D., Guelfo, J.L., 2025. Laboratory validation of a simplified model for estimating equilibrium PFAS mass leaching from unsaturated soils. Sci Total Environ 970, 179036. https://doi.org/10.1016/j.scitotenv.2025.179036.

[89] Wang, H., Nan, Q., Waqas, M., Wu, W., 2022. Stability of biochar in mineral soils: Assessment methods, influencing factors and potential problems. Sci Total Environ 806, 150789. https://doi.org/10.1016/j.scitotenv.2021.150789.

[90] Wang, J., Xiong, Z., Kuzyakov, Y., 2016. Biochar stability in soil: meta-analysis of decomposition and priming effects. GCB Bioenergy 8 (3), 512–523. https://doi.org/10.1111/gcbb.12266.

[91] WHO, 2003. Arsen Drink-Water: Backgr Doc Dev WHO Guidel Drink-Water Qual (WHO/SDE/WSH/03 04/75).

[92] WHO, 2020. Chromium Drink-Water - Backgr Doc Dev WHO Guidel Drink-Water Qual (WHO/SDE/WSH/03 04/04).

[93] Yan, P.-F., Dong, S., Pennell, K.D., Cápiro, N.L., 2024. A review of the occurrence and microbial transformation of per- and polyfluoroalkyl substances (PFAS) in aqueous film-forming foam (AFFF)-impacted environments. Sci Total Environ 927, 171883. https://doi.org/10.1016/j.scitotenv.2024.171883.

[94] Yu, O.-Y., Raichle, B., Sink, S., 2013. Impact of biochar on the water holding capacity of loamy sand soil. Int J Energy Environ Eng 4 (1), 44. https://doi.org/10.1186/2251-6832-4-44.

[95] Zhang, P., Duan, W., Peng, H., Pan, B., Xing, B., 2022. Functional Biochar and Its Balanced Design. ACS Environ Au 2 (2), 115–127. https://doi.org/10.1021/acsenvironau.1c00032.

[96] Zhang, Y., Thomas, A., Apul, O., Venkatesan, A.K., 2023. Coexisting ions and long-chain per- and polyfluoroalkyl substances (PFAS) inhibit the adsorption of short-chain PFAS by granular activated carbon. J Hazard Mater 460, 132378. https://doi.org/10.1016/j.jhazmat.2023.132378.

[97] Zhi, Y., Liu, J., 2016. Surface modification of activated carbon for enhanced adsorption of perfluoroalkyl acids from aqueous solutions. Chemosphere 144, 1224–1232. https://doi.org/10.1016/j.chemosphere.2015.09.097.